ANGIOFE: A CONTINUOUS-DISCRETE MODEL OF ANGIOGENESIS THAT COUPLES VESSEL GROWTH TO MATRIX DEFORMATION

Lowell T. Edgar[1, 3], Steve A. Maas[3], James E. Guilkey[2, 3], Jeffrey A. Weiss[1, 3]

ABSTRACT

Mechanical interactions between angiogenic microvessels and the extracellular matrix (ECM) regulate microvascular topology, but the mechanisms are poorly understood. Microvessel growth, branching and anastomosis are sensitive to properties of the ECM such as fiber orientation, boundary conditions and matrix density. These properties are changed by matrix deformation as neovessel sprouts apply traction forces during growth. Previously, we developed a growth model that accurately predicts network topology in a 3D in vitro model of angiogenesis. In the present study, this model was extended to develop AngioFE, a computational framework that couples the growth model to the simulation of solid mechanics with FEBio (www.febio.org). Each sprouting capillary tip was assigned a cellular traction force, represented by a position- and deformation-dependent body force that was localized around the sprout tip. FEBio was used to solve for deformation of the construct in response to the cellular traction forces. The predicted deformation was used to update microvessel positions, ECM fiber orientation and matrix density. When simulating growth within a 3D collagen gel with the long-axis of the gel constrained, the framework provided realistic predictions of the deformed gel geometry, microvascular alignment and collagen fiber orientation. AngioFE was capable of predicting aligned vasculature within a partially constrained matrix based only on the inhomogeneous deformation of the surrounding ECM. In summary, AngioFE provides a flexible modeling framework to investigate the mechanisms that couple matrix deformation and angiogenic growth.

INTRODUCTION

During angiogenesis, new vascular elements arise by sprouting from existing vasculature. Sprouting endothelial cells apply traction to the ECM, degrade the basement membrane and migrate along components of the extracellular matrix (ECM) (1-3), resulting in neovessel elongation. The ECM serves as the major pathway for mechanotransduction between contact-dependent cells, and therefore the material properties of the ECM determine the stress field that is experienced by neovessels. Changes to the ECM fiber orientation, boundary conditions and matrix density affect the topology of the vascular network (4-8), presumably by modifying mechanical interactions between neovessel sprouts and ECM fibers. For example, using a 3D organ culture model of microvessel fragments within a type-I collagen gel, we have shown that different boundary conditions can lead to drastically different vascular topologies (9). When microvessel fragments were cultured in a rectangular gel that was free to contract, new sprouts formed a randomly oriented network (5, 6, 9). When the long-axis of the gel was constrained to prevent contraction, microvessels and collagen fibers aligned along the constrained axis (6, 9).

The mechanisms that control how global boundary conditions regulate the topology of the vascular network during angiogenesis are poorly understood. The lack in understanding of these mechanisms arises predominately from the difficultly in establishing cause-effect relationships across length scales in the laboratory (i.e. conditions prescribed globally affect interactions at the microscale). For this reason, we have turned to computational modeling in order to study the role of microscale mechanics during angiogenesis. We have previously designed a computational

1. Department of Bioengineering, University of Utah, Salt Lake City, UT, USA
2. Department of Mechanical Engineering, University of Utah, Salt Lake City, UT, USA
3. Scientific Computing and Imaging Institute, University of Utah, Salt Lake City, UT, USA

model of angiogenesis which prescribes microvessel behavior based on properties of the ECM (10). This model, termed "angio3d", has been shown to provide accurate predictions of morphometric data describing vascular network topology across changes in matrix fiber orientation and density (10, 11). However, the model assumed that the material properties of the matrix remained constant during the simulation. It has been observed that neovessel sprouts apply traction to the matrix, resulting in condensation and alignment of the collagen fibrils (12). Therefore, the objective of this study was to develop a computational model in which matrix properties that regulate vascular growth were coupled with the deformation caused by remodeling forces. This was accomplished by coupling our growth model software (angio3d) with the finite element (FE) software FEBio (13) in order to include a framework in solid mechanics. After each time step in the growth model, the results provided by FEBio were used to update matrix properties based on the field theories of continuum mechanics.

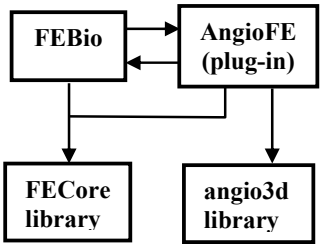

Figure 1. Plug-in framework for FEBio. The FEBio kernel class manages plug-ins. The FECore and angio3d library contains the base classes, which can be subclassed within the plug-in.

METHODS

All software applications were written in C++. The coupling between angio3d and FEBio was accomplished through AngioFE, a plug-in file for FEBio (Figure 1). A plug-in is a precompiled library that can be associated with an executable at run time. The FEBio kernel loads the plug-in file at runtime. This framework allows users to include new functionality to FEBio without the need to edit and rebuild the entire source code.

Angio3d was used to predict the updated microvessel geometry at each time step. Angio3d uses information about the ECM to determine vessel morphology during spontaneous angiogenesis. The ECM was represented by a rectilinear hexahedral FE mesh. Field information that influences growth, such as matrix density and fiber orientation, was specified at the nodes of the mesh. Trilinear shape functions were used to interpolate the fields over the elements:

$$\psi(\boldsymbol{x}) = \sum_{j=1}^{8} \psi_j N_j(\boldsymbol{x}) . \qquad [1]$$

In this equation, ψ is a scalar or vector field, ψ_j are the nodal values, N_j is the value of the shape function for node j at the interpolation position, $\boldsymbol{x}$. Microvessels were represented discretely as a collection of end-to-end line segments. Growth was simulated by the addition of new line segments at the active sprout locations. When creating a new vessel segment, ECM field information was interpolated to the sprout location to regulate the growth step. Collagen fiber orientation was used to determine the direction of the new segment, while matrix density was used to determine the segment's length and branching probability. Branching, defined as the sprouting of a new neovessel from an existing vessel, was modeled as a random process. During a time step, each segment generated a number between 0 and 1. If the random number exceeded the branching probability for that segment, the segment formed a branch. Anastomosis, defined as the fusing of two vessels into one, was permitted for any active growth tip within close proximity of another vessel.

The forces generated by neovessels sprouts were represented using a deformation-dependent force field that was defined relative to the position of the sprout tip, $\boldsymbol{x}_s$. For each sprout tip, a body force $\boldsymbol{f}_s$ was applied to the mesh based on the following equation:

$$\boldsymbol{f}_s = a\cos^N\left(\theta/2\right) e^{\left(-b\|r\|\right)} \hat{\boldsymbol{r}} \; ; \quad \boldsymbol{r} = \boldsymbol{x}_s - \boldsymbol{x} \; , \qquad [2]$$

where a, b, and N are adjustable parameters and $\boldsymbol{r}$ is the vector from $\boldsymbol{x}_s$ to the position $\boldsymbol{x}$ of a point inside the mesh. The angle θ is defined between $\boldsymbol{r}$ and the orientation vector of the parent sprout, $\boldsymbol{n}$ (Figure 2). After all sprout forces were calculated and interpolated to the nodes of the FE mesh, FEBio was used to solve for the resulting deformation field. The material behavior of the vascularized collagen gel was represented with a composite constitutive model. The total Cauchy stress $\boldsymbol{\sigma}$ was the weighted sum of the stress response from the ECM ($\boldsymbol{\sigma}_{ECM}$) and the microvessels ($\boldsymbol{\sigma}_m$):

$$\boldsymbol{\sigma} = \phi\boldsymbol{\sigma}_m + (1-\phi)\boldsymbol{\sigma}_{ECM}\ , \qquad [3]$$

where ϕ is the volume fraction of the microvessels in the element. A hyperelastic constitutive model based on a uniform continuous fiber distribution was used to represent the ECM (14). This model captures the major features of the material properties of collagen gels, including nonlinear elasticity, low modulus in compression and strain-dependent Poisson's ratio (14, 15). The zero-strain tensile Young's modulus was chosen as 24.3 KPa in tension (16) and the compressive Young's modulus was two orders of magnitude smaller (0.243 KPa). We observed that this disparity was essential for realistic predictions of ECM deformation. A transversely isotropic neo-Hookean constitutive model was used to represent the stress contribution from the microvessels. This constitutive model contributed stress only due to deformation along the average microvessel orientation, with a Young's modulus of 20.0 KPa.

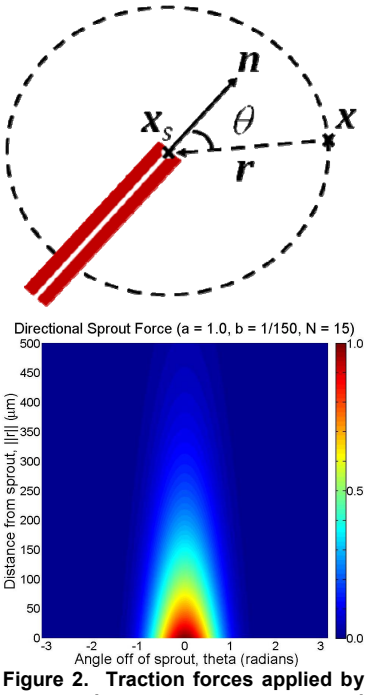

Figure 2. Traction forces applied by neovessel sprouts were represented using a local body force. (Top) Diagram of the sprout representation presented in Eq. 2. (Bottom) Fringe plot of the force field calculated using Eq. 2.

The total stress in the composite was assumed be dissipative, causing deformation in response to cell-generated tractions forces to become permanent (17). Given the large water content within collagen gels, it is reasonable to assume that stress is dissipative rather than accumulative (18, 19). The time-varying second Piola-Kirchhoff stress $\boldsymbol{S}(t)$ was defined by the convolution integral:

$$\boldsymbol{S}(t) = \int_0^t G(t-s)\frac{d\boldsymbol{S}^e}{ds}ds\ ; \qquad G(t) = e^{-\frac{t}{\tau}}, \qquad [4]$$

where the elastic stress $\boldsymbol{S}^e$ is the pull-back of Cauchy stress $\boldsymbol{\sigma}$ as determined from Eqn. [3], and $G(t)$ is the reduced relaxation function. The relaxation constant τ was set at 0.129 days. Once the FE problem was solved using FEBio, the solution was used to update microvessel positions, ECM fiber orientation and matrix density. ECM fiber orientation vectors were treated as free vectors and updated using the deformation gradient tensor. Matrix density was updated based on the conservation of mass using the Jacobian of the deformation gradient.

To demonstrate the capabilities of AngioFE, we simulated angiogenic growth and the associated ECM deformation within a vascularized collagen gel subjected to two different boundary conditions: unconstrained (U) and long-axis constrained (LAC). For these simulations, the sprout force parameters were prescribed as follows: a=2.5x10^7 μm/s^2, b=150 1/μm, and N=15. These values were chosen to obtain a realistic deformation of the gels using the material parameters described above. The dimensions of the ECM domain were 10.25×2.75×1.50 mm. The domain was seeded with 1480 microvessel fragments at initialization, based on the microvessel seeding density of 35,000 fragments/ml used in our comparable experiments (9). Each node was initialized with a random collagen fiber orientation and a matrix density of 3.0 mg/ml. Six days of growth were simulated (9). The predicted Green-Lagrange strain was determined in each direction at the center of the deformed gels. The morphometry of the microvessels was determined for a 2.55×2.55×0.75 mm region at the center of the deformed gels.

To assess alignment, we determined the angle between each microvessel and the long-axis (x-axis). These predictions were compared to similar measurements from the experimental cultures of U and LAC collagen gels (9). After 6 days, the culture dimensions were collected and used to calculate Green-Lagrange strain. Confocal microscopy was used to image microvessels within the constructs. The confocal data sets were skeletonized, and the distribution of angles that each vessel formed with the long-axis (x-axis) was determined.

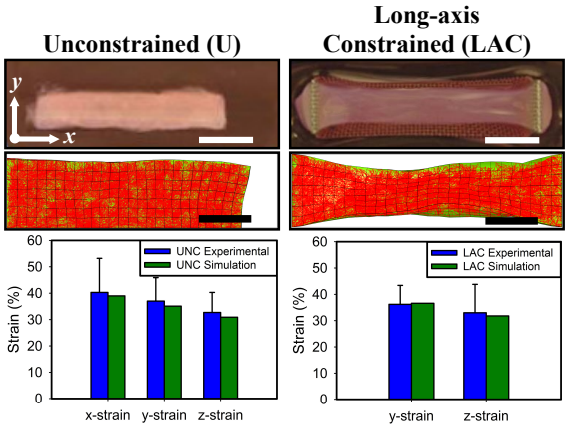

Figure 3. Results for the U boundary condition are presented on the left, results for the LAC boundary condition on the right. (Top) Images of vascularized collagen gels (White scale bar = 5 mm). (Middle) Deformed mesh geometry of the each boundary condition (Black scale bar = 2 mm). (Bottom) Green-Lagrange strain measured from experimental cultures is presented in blue, strain measurements predicted by AngioFE is presented in green. Error bars in the experimental data sets indicate standard deviation (N = 7).

RESULTS

The predictions of the U and LAC geometry were in good agreement with the experimentally measured geometry (Figure 3, top and middle rows). There was good agreement between the strains predicted by Angio FE and the average experimental strains, although strains predicted by AngioFE were slightly lower.

Constraining the long-axis of the gel drastically altered vascular topology. Microvessels within the U gels were randomly oriented, while vessels within the LAC gels were aligned along the constrained axis (Figure 4, top row). AngioFE predicted this behavior. For the U boundary condition, the predicted microvessel orientation was random. In contrast, for the LAC boundary condition, microvessels were preferentially aligned with the long-axis (Figure 4, middle and bottom rows).

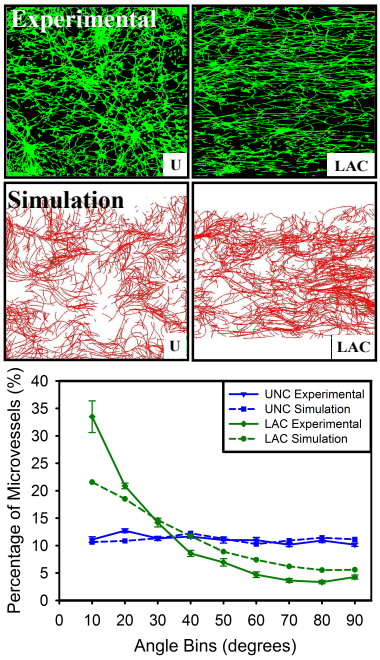

Figure 4. (Top) Confocal images demonstrate that microvessels become preferentially aligned by altering gel boundary conditions. (Middle) Predictions of microvasculature orientation. (Bottom) Predicted angles between microvessels and long-axis of gel closely matched experimental measurements.

DISCUSSION

AngioFE produced realistic predictions of both the deformed geometry and the distribution of microvessel orientation angles for both the U and LAC boundary conditions. These predictions were produced by assigning a body force to active sprout tips within a validated growth model (10, 11). The parameters for the material models and sprout force representation were chosen to produce realistic deformations of the collagen gels, quantified by measuring strain values. In particular, the disparity in stiffness between compressive and tensile loading was necessary for realistic predictions. For example, if the ECM was represented by a neo-Hookean material instead of the continuous fiber distribution material, the simulations predicted excessive torsion and buckling of the gels.

In this simulation framework, microvessel alignment arises solely due to the deformation of the mesh (ECM). This design makes the model ideal for investigating the relationship between matrix deformation and microvessel orientation during angiogenesis. In the unconstrained

simulation, the mesh was free to deform in each direction. Since the microvasculature was coupled with the deformation of the mesh through the displacement field, the line segments representing microvessels were also free to contract in each direction equally and therefore no preferential alignment emerged within this boundary condition. The constraints placed on the mesh while simulating the LAC boundary condition caused the mesh to be free to deform only in the y- and z- direction. Therefore, line segments within the simulation contracted along these directions, while their length along the x-direction was unchanged. The alignment in the LAC simulations was caused by this anisotropic deformation field. These results are supported by observations that anisotropic compressive strain loading of cell-populated collagen gels causes alignment of both matrix fibers and cells perpendicular to the direction of contraction (19-23). These results suggest that passive re-orientation of microvessels by an anisotropic deformation field arising due to the gel boundary conditions can result in preferential microvessel alignment.

Several assumptions of the model likely have a strong influence on the predictions. Although AngioFE was capable of predicting preferential alignment of microvasculature using the matrix deformation field, alignment in the LAC simulation was not as pronounced as has been observed *in vitro*. Passive re-orientation of microvessels may be capable of producing significant alignment, but there may be an active response to the changing matrix environment that causes growing microvessels to further align along the constrained axis (24). Further, simulations assumed that the matrix and microvessels experienced the same deformation field, i.e. their deformations were compatible. However, the deformation fields for cells and collagen fibrils within cell seeded constructs are incompatible (25-27), and allowing for incompatible deformation might produce better agreement with the experiments. Another assumption in the model that requires further investigation is the specific force field that was assumed for the sprout force. Other representations of the force field could alter mesh deformation and may lead to more accurate predictions. For example, FE models using a uniform pressure to drive contraction of the matrix have been shown produce accurate predictions of microvascular alignment (9, 28).

Despite these considerations, AngioFE was capable of predicting aligned vasculature within a partially constrained matrix based only on the inhomogeneous deformation of the surrounding ECM. The model does not require meshing of the intricate microvessel geometry or the interface between vessels and the ECM. Micromechanical interactions between vessels and ECM fibrils were accounted for in an averaged sense by treating the vascularized gel as a continuum. In the future, AngioFE can be used to simulate other boundary conditions and further elucidate these mechanisms. This framework may also be able to predict regions of high and low stress within the microvessels, which may result in the formation of a new branch or the regression of an existing neovessel respectively (29). Applications in tissue engineering include the design of optimized vascular topologies for pre-vascularized implants. In summary, AngioFE provides a flexible modeling framework to investigate the mechanisms that couple matrix deformation and angiogenic growth.

ACKNOWLEDGEMENTS

This work was supported by the National Institutes of Health (HL077683).

REFERENCES

1. Fisher, C., Gilbertson-Beadling, S., Powers, E. A., Petzold, G., Poorman, R., and Mitchell, M. A., Interstitial collagenase is required for angiogenesis in vitro, Dev. Biol., 1994, Vol. 162, 499-510.
2. Haas, T. L., Davis, S. J., and Madri, J. A., Three-dimensional type I collagen lattices induce coordinate expression of matrix metalloproteinases MT1-MMP and MMP-2 in microvascular endothelial cells, J. Biol. Chem., 1998, Vol. 273, 3604-3610.
3. Vernon, R. B. and Sage, E. H., A novel, quantitative model for study of endothelial cell migration and sprout formation within three-dimensional collagen matrices, Microvasc. Res., 1999, Vol. 57, 118-133.
4. Shiu, Y.T., Weiss, J., Hoying, J., Iwamoto, M., Joung, I., and Quam, C.T., The role of mechanical stresses in angiogenesis, Crit. Rev. Biomed. Eng., 2005, Vol. 33, 431 - 510.

5. Krishnan, L., Hoying, J., Nguyen, H., Song, H. and Weiss, J., Interaction of angiogenic microvessels with the extracellular matrix, Am. J. Physiol. Heart Circ. Physiol., 2007, Vol. 293, H3650 – H36588.
6. Krishnan, L., Underwood, C., Maas, S., Ellis, B., Kode, T., Hoying, J., and Weiss, J., Effect of mechanical boundary conditions on orientation of angiogenic microvessels, Cardiovasc. Res., 2008, Vol. 78, 324 - 332.
7. Ghajar, C., Chen X., Harris J., Suresh V., Hughes C., Jeon N., Putnam A., and George, S., The effect of matrix density on regulation of 3-D capillary morphogenesis, Biophys. J., 2008, Vol. 94, 1930 - 1941.
8. Sieminski, A., Hebbel R., and Gooch, K., The relative magnitudes of endothelial force generation and matrix stiffness modulate capillary morphogenesis in vitro, Exp. Cell Res., 2004, Vol. 297, 574 – 584.
9. Underwood, C., Krishnan, L., Edgar, L.T., Maas, S., Hoying, J., and Weiss, J., The effects of geometry and static boundary conditions on microvessel outgrowth in a 3D model of angiogenesis, Proc. ASME SBC 2010.
10. Edgar, L.T., Sibole, S., Underwood, C., Guilkey, J., and Weiss, J., A computational model of in vitro angiogenesis based on extracellular matrix fiber orientation, Comp. Meth. Biomech. Biomed. Eng., 2011, In Press.
11. Edgar, L.T., Sibole, S., Underwood, C., Guilkey, J., and Weiss, J., Simulating the influence of the extracellular matrix on 3D in vitro angiogenesis, Proc. CMBBE 2010.
12. Kirkpatrick, N. D., Andreou, S., Hoying, J.B., and Utzinger, U., Live imaging of collagen remodeling during angiogenesis, Am. J. Physiol. Heart Circ. Physiol., 2007, Vol. 292, H3198-3206.
13. Maas, S., Ellis, B., Ateshian, G., and Weiss, J., FEBio: Finite elements for biomechanics, J. Biomech. Eng., 2011, Vol. 134. (FEBio is available for download at www.febio.org).
14. Ateshian, G., Rajan, V., Chahine, N., Canal, C., and Hung, C., Modeling the matrix of articular cartilage using a continuous fiber angular distribution predicts many observed phenomena, J. Biomech. Eng., 2009, Vol. 131.
15. Roeder, B., Kokini, K., and Voytik-Harbin, S., Fibril microstructure affects strain transmission within collagen extracellular matrices, J. Biomech. Eng., 2009, Vol. 131.
16. Roeder, B., Kokini, K., Sturgis, J., Robinson, J.P., and Voytik-Harbin, S., Tensile mechanical properties of three-dimensional type I collagen extracellular matrices with varied microstructure, J. Biomech. Eng., 2002, Vol. 124.
17. Puso, M., and Weiss, J., Finite element implementation of anisotropic quasilinear viscoelasticity using a discrete spectrum approximation, J. Biomech. Eng., 1998, Vol. 120.
18. Krishnan, L., Weiss, J., Wessman, M., and Hoying, J., Design and application of a test system for viscoelastic characterization of collagen gels, Tiss. Eng., 2004, Vol. 10, 241-252.
19. Chandran, P., and Barocas, V., Microstructural mechanics of collagen gels in confined compression: poroelasticity, viscoelasticity, and collapse, J. Biomech. Eng., 2004, Vol. 126.
20. Girton, T., Barocas, V., and Tranquillo, R.T., Confined compression of a tissue-equivalent: collagen fibril and cell alignment in response to anisotropic strain, J. Biomech. Eng., 2002, Vol. 124.
21. Tranquillo, R.T, Self-organization of tissue-equivalents: the nature and role of contact guidance, Biochem. Soc. Symp., 1999, Vol. 65, 27-42.
22. Martinez, H., Brackmann, C., Enejder, A., and Gatenholm, P., Mechanical stimulation of fibroblasts in micro-channeled bacterial cellulose scaffolds enhances production of oriented collagen fibers, J. Biomed. Mat. Res. A, 2012, Vol. 100, 948-957.
23. Costa, K.D., Lee, E. J., and Holmes, J. W., Creating alignment and anisotropy in engineered heart tissue: role of boundary conditions in a model three-dimensional culture system, Tiss. Eng., 2003, Vol. 9, 567-577.
24. Gefen, A., Cellular and biomolecular mechanics and mechanobiology, 2011, Springer.
25. Chandran, P., and Barocas, V., Affine versus non-affine fibril kinematics in collagen networks: Theoretical studies of network behavior, J. Biomech. Eng., 2006, Vol. 128.
26. Hepworth, D., Steven-fountain, A., Bruce, D., and Vincent, J., Affine versus non-affine deformation of soft biological tissues, measured by the reorientation and stretching of collagen fibres through the thickness of compressed porcine skin, J. Biomech., 2001, Vol. 34, 341-346.
27. Ulrich, T., Jain, A., Tanner, K., MacKay, J., and Kumar, S., Probing cellular mechanobiology in three-dimensional culture with collagen-agarose matrics, Biomat., 2010, Vol. 31, 1875-1884.
28. Chang, C.C., Krishnan, L., Nunes, S.S., Church, K.H., Edgar, L.T., Boland, E.D., Weiss, J.A., Williams, S.K., Hoying, J.B., Determinants of microvascular network topology in implanted neovasculatures, Arterioscler. Thromb. Vasc. Biol., 2011, Vol. 32, 5-14.
29. Ingber, D.E., Mechanical signaling and the cellular response to extracellular matrix in angiogenesis and cardiovascular physiology, Circ Res, 2002, Vol. 91, 877-87.